ACS APPLIED MATERIALS & INTERFACES

Research Article

www.acsami.org

Silver Nanowire/Optical Adhesive Coatings as Transparent Electrodes for Flexible Electronics

Michael S. Miller, Jessica C. O'Kane, Adrian Niec, R. Stephen Carmichael, and Tricia Breen Carmichael*

Department of Chemistry and Biochemistry, University of Windsor, Windsor, Ontario, Canada N9B 3P4

ABSTRACT: We present new flexible, transparent, and conductive coatings composed of an annealed silver nanowire network embedded in a polyurethane optical adhesive. These coatings can be applied to rigid glass substrates as well as to flexible polyethylene terephthalate (PET) plastic and elastomeric polydimethylsiloxane (PDMS) substrates to produce highly flexible transparent conductive electrodes. The coatings are as conductive and transparent as indium tin oxide (ITO) films on glass, but they remain conductive at high bending strains and are more durable to marring and scratching than ITO. Coatings on PDMS withstand up to 76% tensile strain and 250 bending cycles of 15% strain with a negligible increase in electrical resistance. Since the silver nanowire network is embedded at the surface of the optical adhesive, these coatings also provide a smooth surface (root mean squared surface roughness <10 nm), making them suitable as transparent conducting electrodes in flexible light-emitting electrochemical cells. These devices continue to emit light even while being bent to radii as low as 1.5 mm and perform as well as unstrained devices after 20 bending cycles of 25% tensile strain.

KEYWORDS: *flexible electronics, nanowires, organic electronics, electrodes, functional coatings*

INTRODUCTION

Flexible displays of organic light-emitting devices (OLEDs) on lightweight plastics are nearing commercial reality.[1] Despite years of research and development, however, the flexibility of these displays is still limited by reliance on the transparent conductor indium tin oxide (ITO).[2] ITO is universally used in rigid optoelectronic devices, but it is completely unsuitable for flexible devices because it is a brittle ceramic. Here, we describe a new transparent conductive coating of silver nanowires (AgNWs) embedded in a transparent polyurethane optical adhesive (OA) that can be applied to a variety of substrates—rigid glass, flexible polyethylene terephthalate (PET), and even elastomeric polydimethylsiloxane (PDMS). AgNW-OA coatings not only rival the conductivity (sheet resistance <20 Ω/□) and transparency (>85%) of ITO[3] but also surpass ITO in flexibility and durability. We demonstrate their use as electrodes in flexible light-emitting electrochemical cells (LEECs) and show that repeated bending does not affect the device properties.

Devices fabricated on lightweight, flexible plastics open the way to thin, lightweight displays, large-area lighting panels, and solar cells that can be rolled, folded, or mounted on curved surfaces. Flexibility requires that each layer of these thin-film devices—metal electrodes, transparent conductive electrodes (TCEs), active organic materials, and device interconnects—functions under bending strains. We cannot rely on the universal standard TCE used in rigid optoelectronics—ITO—because it compromises both the electrical and mechanical performance of flexible devices. ITO films on glass boast low sheet resistance (<20 Ω/□) and high transparency (>85%); however, the sheet resistance of ITO films on PET is higher (60 Ω/□, 80% transparency) due to the low processing temperatures required by plastic substrates.[3] Furthermore, ITO films on flexible plastics crack at relatively low bending strains (2−3%), and repeated bending leads to catastrophic electrical failure.[2] The onus is on the research community to develop drop-in replacements for ITO that can deliver conductivity and transparency as good as ITO on glass, combined with the ability to tolerate repeated cycles of bending. In response, researchers are pursuing a number of alternative TCE materials to replace ITO, such as carbon nanotubes,[4] graphene,[5,6] conductive polymers,[7−9] metallic grids,[10−13] and metallic nanowires.[14−31]

Many view AgNW films as the most promising replacement for ITO, but substantial problems still hinder the adoption of these materials. AgNW networks deposited on substrates by drop-casting,[14,15] meyer rod coating,[17,18] spray coating,[19,20] and vacuum filtration[21,22] display optical and electrical properties similar to ITO and retain conductivity while bent; however, there are two crucial drawbacks that limit the use of these AgNW films in real devices. First, many of these techniques produce AgNW films that are not adhered to the substrate, making them fragile and easily displaced.[25] Second, these AgNW films consist of an irregular pile of AgNWs with

Received: July 16, 2013
Accepted: September 5, 2013
Published: September 5, 2013

individual AgNWs protruding >100 nm from the surface. Since the films comprising thin-film devices are often ~100 nm in thickness, protruding AgNWs provide pathways for electrical shorts and thus are unsuitable for use as electrodes.[15,18]

Embedding AgNWs into polymer films is a promising way to improve adhesion and reduce height variation at the surface. Two methods have been reported: The first method embeds the AgNWs into the surface of specific polymeric substrates, such as polyvinyl alcohol (PVA)[25] or crosslinked polyacrylate.[27] The second method embeds the AgNWs in an un-cross-linked polymer layer, such as poly(3,4-ethylenedioxythiophene) poly-(styrenesulfonate) (PEDOT:PSS), on top of a plastic substrate.[14] Both methods produce AgNW composites with conductivity and transparency competitive with ITO/PET or ITO/glass, low surface roughness of <10 nm, and minimal increases in resistance after bending. Despite these impressive developments, these AgNW composites cannot yet be called drop-in replacements for ITO. ITO is a coating that can be applied to different substrates (e.g., PET, polyethylene naphthalate, polyimide),[3] as well as plastics treated with multilayer barrier coatings that are essential to reduce the permeation of moisture and air, which degrade organic electronic materials and severely limit operating device lifetime.[32] ITO is also impervious to common solvents used to deposit thin films of device materials by spin coating, making it compatible with low-cost solution processing. In contrast, existing AgNW composite films each lack at least one of these important features. AgNW films embedded in specific polymer substrates will need to be integrated with gas-impermeable plastics to be useful for practical flexible organic electronics. These polymer substrates also may not have the desired mechanical properties. For example, polyacrylate substrates with embedded AgNWs must be heated to above the glass transition temperature (110 °C) for them to be flexible or stretchable.[26,27] AgNWs embedded in un-cross-linked polymers such as PEDOT:PSS[14] or PVA[25] also may not be compatible with solution processing of device thin films due to possible dissolution of the polymer in the solvent.

Our approach to flexible and transparent electrodes is to fabricate a coating consisting of an annealed AgNW film embedded in a transparent polyurethane optical adhesive that can be applied to the substrate of choice. The fabrication procedure is simple, is inexpensive, and uses commercially available materials, which makes the coatings easily accessible as transparent electrodes for flexible device testing. The coatings are as conductive and transparent as ITO/glass, with a low surface roughness (<10 nm) that makes them compatible with thin-film devices. Since optical adhesives are designed to bond components together, AgNW-OA coatings adhere to a variety of target substrates. We demonstrate AgNW-OA coatings on glass, PET, and PDMS substrates; these coatings should also be applicable to the impermeable plastics necessary for practical flexible electronics. Optical adhesives are crosslinked polymers, which impart durability and solvent resistance to the AgNW-OA coatings, making them essentially unaffected by marring, scratching, or solvent exposure. They show a negligible increase in resistance after bending to tensile strains as high as 76% or after 250 cycles of bending to 15% tensile strain.

RESULTS AND DISCUSSION

The process to fabricate AgNW-OA coatings on glass, PET, or PDMS substrates combines commercially available AgNWs with a polyurethane optical adhesive according to Scheme 1.

Scheme 1. Process Used to Fabricate AgNW-OA Coatings

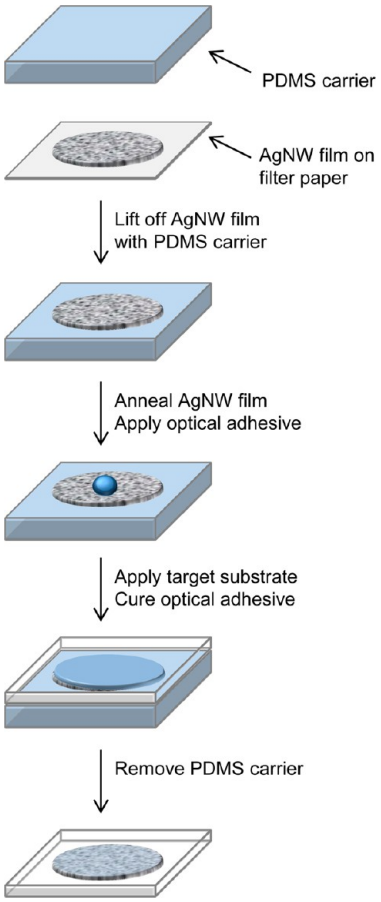

Vacuum filtering a AgNW dispersion in ethanol (0.025 mg/mL) through hydrophobic filter paper produces a uniform AgNW film, which is then transferred to a flat PDMS carrier substrate and annealed to fuse the AgNWs at their intersection points.[16] We form AgNW coatings by depositing a drop (5 μL/cm^2) of optical adhesive onto the surface of the AgNW film on the PDMS carrier and then placing a target substrate (glass, PET, or oxidized PDMS) on top. After curing the adhesive, the PDMS carrier substrate easily peels away to leave the cured AgNW-OA coating adhered to the target substrate. The PDMS carrier plays a significant role in the success of this process: First, PDMS can tolerate the high temperatures (200 °C) required to anneal the AgNW film. Second, the surface free energy of the PDMS carrier is ideal for both transfer processes.[33] It is higher than that of the hydrophobic filter paper, which allows the PDMS carrier to cleanly pick up the AgNW network from the filter paper. It is also lower than that of the target substrates (glass, PET, oxidized PDMS), which enables the release of the AgNW-OA film from its surface to the target substrate. Finally, the PDMS surface provides a smooth template for what is ultimately the surface of the AgNW-OA coating after transfer to the target substrate.

AgNW-OA coatings on all three target substrates are highly transparent and conductive. A photograph of a AgNW-OA coating adhered to PDMS is shown in Figure 1a. By simply varying the volume of the AgNW dispersion passed through the filter paper, we prepared AgNW-OA coatings with sheet resistances of 4 Ω/□, 9 Ω/□, and 14 Ω/□ and transmittances at 550 nm of 81%, 86%, and 89%, respectively. Figure 1b shows the transmission spectra for the AgNW-OA coatings on glass

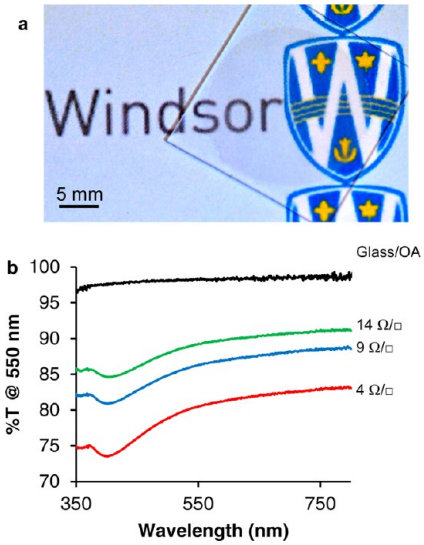

Figure 1. Electrical and optical properties of AgNW-OA coatings. (a) Photograph of a AgNW-OA coating on PDMS (14 Ω/□). (b) Transmittance spectra of AgNW-OA coatings on glass, with corresponding sheet resistances. University of Windsor logo used with permission.

substrates, along with the spectrum of a film of the optical adhesive on glass. A summary of the data for AgNW-OA coatings on glass is provided in Table 1. The 4 Ω/□ and

Table 1. Electrical and Optical Properties of AgNW-OA Coatings on Glass

R_s (Ω/□)	% T (at 550 nm)
14.1 ± 1.6	89.2
8.8 ± 0.5	86.3
3.9 ± 0.2	80.5

9 Ω/□ coatings are as conductive and transparent as ITO/glass and also surpass other AgNW films embedded in polymers reported in the literature.[14,21,25−27] We believe that the low sheet resistance and high transparency exhibited by AgNW coatings are due to annealing the AgNW films, which is known to reduce the sheet resistance. In addition, annealing gives the AgNW film mechanical stability by fusing the AgNWs at their intersection points, allowing the network to be transferred to the target substrate without disruption. Annealing is essential to maintain the integrity of the AgNW network; without the annealing step, the resulting AgNW-OA coatings are not conductive.

Scanning electron microscopy (SEM) and atomic force microscopy (AFM) reveal that AgNW-OA coatings are uniform and smooth. Cross-sectional SEM images of an AgNW-OA (4 Ω/□) coating on glass (Figure 2a and 2b) show that the AgNW network resides at the surface of a ∼25-μm-thick film of optical adhesive adhered to the glass substrate. SEM views of the top of the film (Figure 2c and 2d) show a network of interconnected AgNWs embedded in, and not protruding from, the optical adhesive surface. AFM studies of AgNW-OA (9 Ω/□) films formed on glass, PDMS, and PET substrates showed that the films have similar root-mean-square (RMS) roughness values (6.2, 5.0, and 7.5 nm, respectively) and maximum peak heights of ∼30 nm (Figure 3), indicating that the coating roughness is essentially independent of the substrate. We also

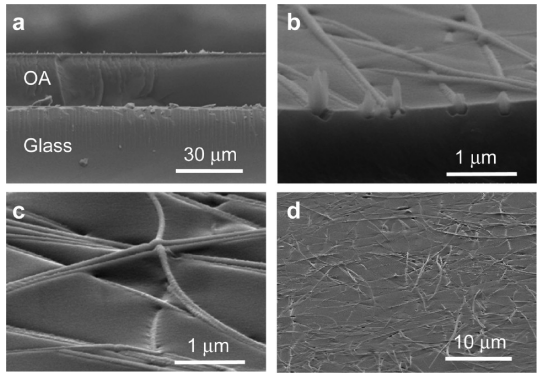

Figure 2. Structural features of AgNW-OA coatings. (a, b) Cross-sectional SEM images of a freeze-fractured AgNW-OA coating on glass (4 Ω/□). (c, d) SEM images of the surface of a AgNW-OA coating (4 Ω/□) on glass.

compared how much the AgNWs protrude from the surface of a AgNW-OA (14 Ω/□) coating on PDMS to AgNW films with a similar AgNW density deposited on a silicon wafer by drop casting.[34] The RMS roughness of the AgNW-OA film is 9.3 nm (Figure 4a), which is an order of magnitude lower than that of the drop-cast AgNW film (42.7 nm, Figure 4c). More importantly, AFM profile measurements (Figure 4b, d) reveal that the variation in maximum height over the scan area for the AgNW-OA film (<25 nm) makes these films suitable for use in thin-film devices. In contrast, AgNWs protrude from the drop-cast film up to 150 nm from the surface of the wafer.

AgNW-OA coatings are remarkably flexible. We measured the change in resistance of AgNW-OA (4 Ω/□) coatings on 75 μm thick PET and 1 mm thick PDMS substrates at various bending radii. A photograph of a bent AgNW-OA film on PDMS is shown in Figure 5a, and Figure 5b shows a plot of the change in resistance versus the tensile strain calculated according to the equation below[35]

$$\varepsilon = d/2r$$

where ε represents the tensile strain; d is the thickness of the substrate; and r is the radius of curvature. Remarkably, bending the films to radii as small as 0.65 mm produced a negligible change in resistance for AgNW-OA coatings on both PET (strain = 5.8 %) and PDMS (strain = 76.9 %). The resistance of AgNW-OA films on PET increases less than 2-fold (R/R_0 = 1.41 ± 0.03) when films are plastically deformed by creasing to a radius of ∼0.1 mm (37.5% tensile strain). In comparison, the resistance of ITO films on PET drastically increases to 88× the original value at 2% tensile strain;[27] that of AgNWs embedded into a polyacrylate substrate increases by 3.9× at 16% tensile strain.[27] The impressive flexibility of AgNW-OA coatings on PDMS substrates, however, does not extend to stretchability. The application of linear strain instead of bending strain produces tearing through the optical AgNW-OA coating and PDMS. This fracturing is likely due to the limited stretchability of the optical adhesive, which has an elastic modulus of 160 000 psi. We are currently investigating the use of stretchable adhesives to replace the current optical adhesive and plan to report these studies in a separate publication. We also tested the ability of AgNW-OA coatings to tolerate repeated bending by measuring the sheet resistance every 10 cycles for 250 cycles of 15% tensile strain (Figure 5c). We measured the sheet resistance in two directions by orienting a four-point probe to inject current parallel to, and then perpendicular to, the

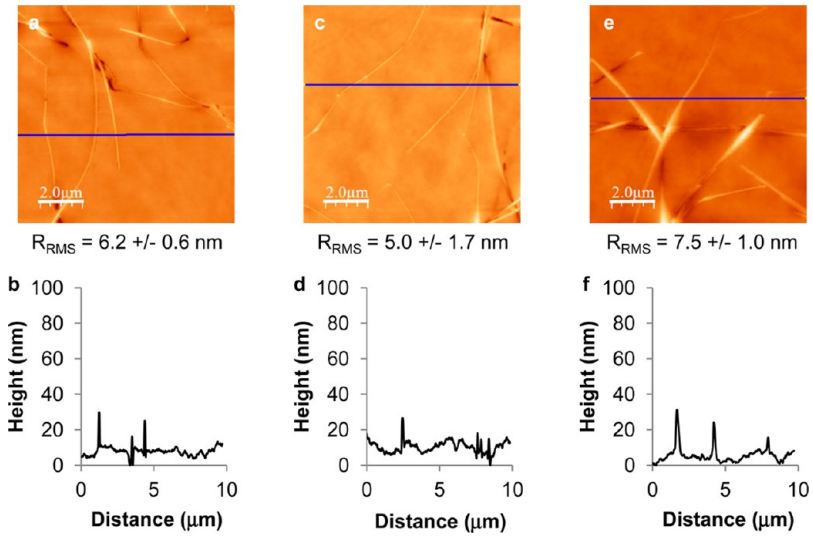

Figure 3. AFM images (z-scale = 150 nm) with root-mean-squared (RMS) roughness measurements and corresponding profile measurements of AgNW-OA films (9 Ω/□) on (a, b) glass; (c, d) PDMS; and (e, f) PET.

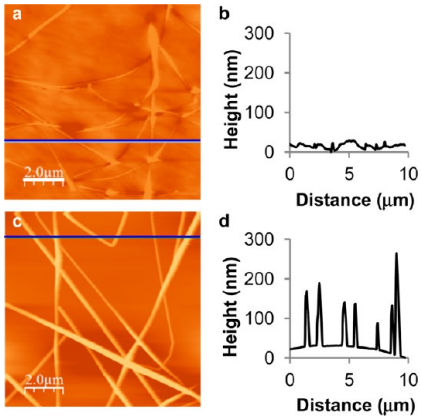

Figure 4. Comparison of surface roughness of AgNW-OA coatings and drop-cast AgNW films. (a, b) AFM image and corresponding profile measurements of a AgNW-OA (14 Ω/□) coating on PDMS. (c, d) AFM image and corresponding profile measurements of a AgNW film on a silicon wafer formed by drop casting.

bending axis. Before bending, there was no difference in resistance in the two directions; however, we observed anisotropy in the resistance that increased with the number of strain cycles. After 250 cycles, the resistance parallel to the bending axis increased to 1.9× the initial value, whereas the resistance perpendicular to the bending axis decreased to 0.5× the initial value. We speculate that bending causes alignment of the AgNWs perpendicular to the bending axis, reducing the resistance. Similar effects have previously been reported for AgNWs deposited onto pre-stretched elastomeric substrates when the strain is released[36] and for carbon nanotube fibers that have been embedded into a polymer matrix and uniaxially stretched.[37,38] Investigation of this possible alignment effect will be reported separately as it is beyond the scope of the present paper.

AgNW-OA coatings adhere strongly to the underlying substrate and are durable to marring, scratching, and solvent exposure. The AgNW-OA coatings pass the tape test without a change in resistance or deposition of observable residue on the adhesive surface of the tape. The resistance also remains constant after vigorous agitation with a gloved finger for 30 s (Table 2). We repetitively clamped and unclamped alligator clips with serrated edges to compare the effect of scratching on AgNW-OA coatings on glass to ITO/glass. Figure 6a shows a photograph of the alligator clips used for the testing clamped to a AgNW-OA film on glass; dark-field optical micrographs in Figures 6b and 6c show the scratches on a AgNW-OA film on glass and an ITO film on glass, respectively, after 100 cycles of clamping and unclamping with the alligator clips. The resistance of AgNW-OA coatings on glass after cycles of repetitive clamping and unclamping of the same area of the film remained relatively constant through the testing cycles; after 200 cycles there was essentially no change in the resistance (R/R_o = 1.23). In contrast, the resistance of ITO films on glass showed greater variation in resistance with the testing cycles and a trend of increasing resistance. After 200 cycles, the resistance of the ITO film increased from 48 to 93 Ω. Finally, we tested the effect of solvent exposure on AgNW-OA coatings on PDMS by immersion in water and ethanol for six hours. Similar to the other durability tests, solvent immersion had little effect on the resistance of the coating (Table 2).

To demonstrate that the characteristics of AgNW-OA coatings make them well-suited for use in flexible devices, we fabricated flexible LEECs using AgNW-OA (14 Ω/□) films on PDMS as the transparent anode and characterized the devices before and after cycles of bending. We chose the LEEC as our test structure due to its simple device architecture, which consists of a mixture of ionic and electronic conductors sandwiched between two metal electrodes.[39,40] The anode, cathode, and emissive layer support all three processes of charge injection, charge transport, and emissive recombination due to enhancement of charge injection that occurs at the electrodes.[40−44] This enhancement makes additional electron/hole injection, transport, and blocking layers unnecessary. The simplicity of the LEEC architecture has previously been exploited in the fabrication of intrinsically bendable and stretchable devices.[27,30,45−47] We fabricated flexible LEECs according to the device structure depicted in Scheme 2. The device consisted of the AgNW-OA anode with a spin-coated layer of PEDOT:PSS on the surface. The emissive layer was the ionic transition metal complex, $Ru(dtb\text{-}bpy)_3(PF_6)_2$, dispersed in poly(methyl methacrylate) (PMMA). A drop of liquid

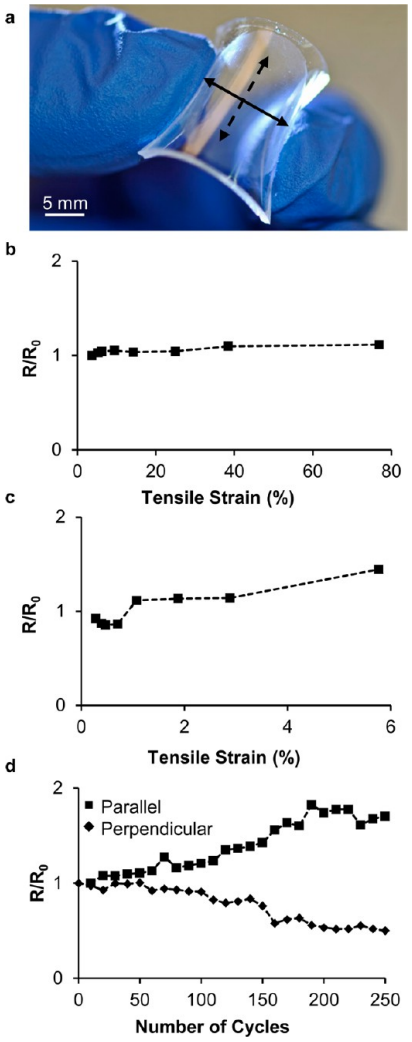

Figure 5. AgNW-OA coatings subjected to bending. (a) Photograph of a flexed AgNW-OA coating (14 Ω/□) on PDMS. The solid line indicates that axis of bending; the dashed line indicates the perpendicular axis. (b) Change in resistance of AgNW-OA coatings (4 Ω/□) on PDMS as a function of increasing tensile strain. (c) Change in resistance of AgNW-OA coatings (4 Ω/□) on PET as a function of increasing tensile strain. (d) Change in resistance of AgNW-OA coatings (4 Ω/□) on PDMS with repetitive cycles of 15% tensile strain measured with a four-point probe oriented to inject current along the bending axis (squares) and along the perpendicular axis (diamonds).

Table 2. Change in Resistance of AgNW-OA Films (4 Ω/□) on PDMS Subjected to Durability Tests

	adhesive tape	finger friction	immersion in water	immersion in EtOH
R/R_o	1.02 ± 0.02	0.99 ± 0.03	0.93 ± 0.10	0.97 ± 0.15

gallium–indium eutectic (EGaIn) served as the cathode to complete the device. Unstrained devices produced bright, uniform emission over the entire area defined by the cathode. These devices continued to emit light when bent to radii of 7.0, 3.0, and 1.5 mm (Figure 7). We compared the device characteristics of unstrained devices to devices subjected to 20 bending cycles of 25% tensile strain by recording the temporal evolution of current and radiance of the devices during ten minutes of operation at 5 V in ambient conditions

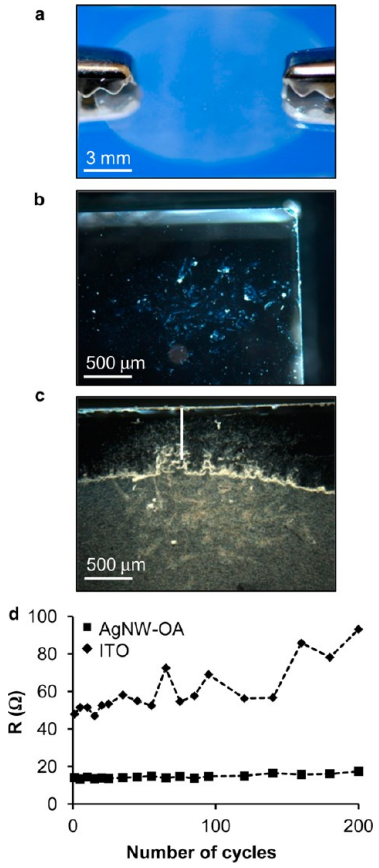

Figure 6. (a) Photograph of serrated alligator clips clamping onto a AgNW-OA (4 Ω/□) coating on glass. (b) Dark-field optical micrograph showing ITO on glass after 100 clamping cycles. (c) Dark-field optical micrograph showing a AgNW-OA (4 Ω/□) coating on glass after 100 clamping cycles. (d) Resistance of AgNW-OA (4 Ω/□) coatings on glass (squares) and ITO on glass (diamonds) measured after repetitive cycles of clamping and unclamping the same area with alligator clips.

Scheme 2. Diagram of the Device Test Structure

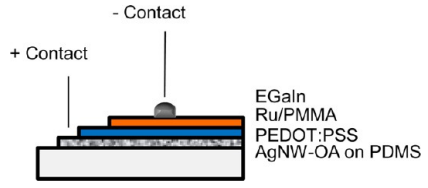

and calculating the external quantum efficiencies (EQE) for the unstrained (Figure 8a and 8b) and strained devices (Figure 8c and d). Both devices reached their maximum EQE by <90 s, followed by a decay in radiance over the testing period due to ambient moisture that degrades the ionic transition metal emitter.[48] Maximum EQEs of unstrained (0.57%) and strained (0.82%) devices fall within the range of EQEs (0.4–0.9%) reported for LEECs with the same emissive layer, an ITO anode on glass, and a gold laminated top contact.[49] Bending cycles thus do not negatively impact the device performance, indicating that the strain does not damage the components of the flexible LEECs.

dx.doi.org/10.1021/am402847y | ACS Appl. Mater. Interfaces 2013, 5, 10165–10172

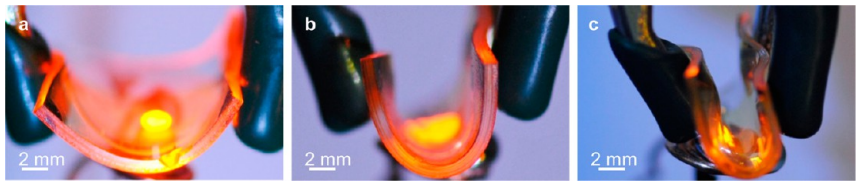

Figure 7. Photographs of flexible LEECs fabricated with AgNW-OA (14 Ω/□) transparent anodes on PDMS, bent to radii of (a) 7.0 mm; (b) 3.0 mm; and (c) 1.5 mm.

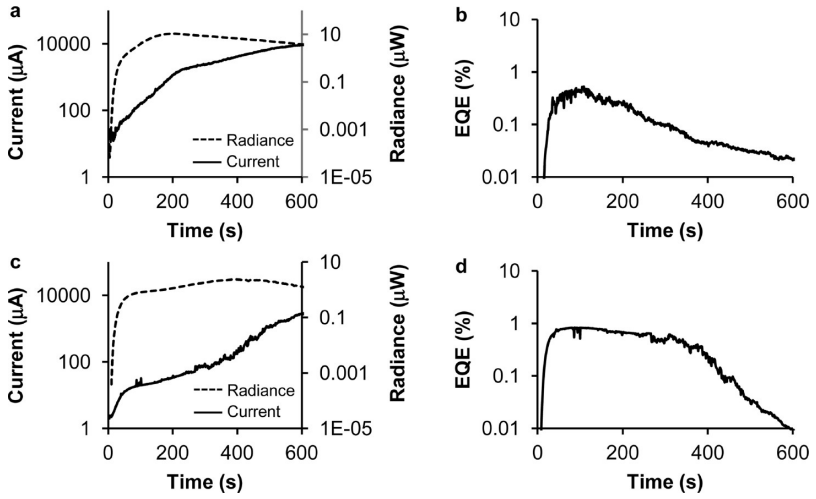

Figure 8. Characterization of unstrained devices and devices subjected to cycles of tensile strain. (a) Temporal evolution of current (solid line) and radiance (dotted line) of a typical unstrained device operated under a 5 V bias in ambient conditions. (b) Temporal evolution of EQE of a typical unstrained device operated under a 5 V bias in ambient conditions. (c) Temporal evolution of current (solid line) and radiance (dotted line) of a typical device after 20 bending cycles of 25% tensile strain operated under a 5 V bias in ambient conditions. (d) Temporal evolution of EQE of a typical device after 20 bending cycles of 25% tensile strain operated under a 5 V bias in ambient conditions.

CONCLUSIONS

Finding transparent conductive films to replace ITO is a highly active field of research that has generated a large body of literature. However, a successful replacement for ITO in flexible electronics must combine a number of essential features—high transparency, low sheet resistance, low surface roughness, good conductivity at high strains, and durability to repetitive strain—as well as being inexpensive and simple to fabricate. We believe that AgNW-OA coatings can be instrumental in the development of flexible electronic devices because these coatings not only possess all of the essential features but also use simple, commercially available materials in a straightforward and inexpensive fabrication scheme that can be applied to different flexible substrates, which potentially includes the highly impermeable plastics crucial to the development of flexible organic electronics. The ease of preparation and versatility of AgNW-OA coatings means they can easily be adopted by other research labs as flexible transparent electrodes to study new flexible electronic devices. Here, we have demonstrated their use as transparent electrodes in LEECs to show that the crosslinked optical adhesive of AgNW-OA coatings makes them compatible with the solvents used to fabricate the thin-film devices. Currently, the ideal application for AgNW-OA coatings is in lab-scale test structures due to the size of the AgNW-OA coatings that can be produced using the method described here, which is limited by the size of the filtration apparatus used to produce the initial AgNW network. We are currently developing methods to broaden the applicability of AgNW-OA coatings beyond the research lab by producing large-area AgNW networks that are compatible with our protocol for transferring and embedding in optical adhesive.

METHODS

Preparation of Glass, PET, and Oxidized PDMS Substrates. Glass microscope slides (VWR) and PET films (Goodfellow, thickness = 75 μm) were cut into 2 cm × 2 cm squares, sonicated (Branson model 3510) for 10 min in deionized water, acetone, and then isopropanol, and dried under a stream of nitrogen. Clean PET films were adhered to a glass microscope slide using double-sided tape (3M). PDMS substrates were fabricated by casting liquid pre-polymer (Sylgard 184, Dow Chemical) against flat polystyrene Petri dishes and curing overnight in a 60 °C oven. Cured PDMS films were cut into 2 cm × 2 cm squares, removed from the Petri dish, and oxidized in air plasma (Harrick Plasma) for 40 s. Oxidized PDMS substrates were then rinsed with methanol and dried under a stream of nitrogen.

Fabrication of AgNW-OA Films on Glass, PET, and Oxidized PDMS. Silver nanowires with an average diameter of 90 nm and average length of 25 μm dispersed in ethanol (10 mg/mL, SLV-NW-90, BlueNano Inc.) were diluted to 0.025 mg/mL with ethanol and then ultrasonicated for 45 s. The desired volume of dilute AgNW solution was filtered through a piece of filter paper (Millipore Durapore Hydrophobic 0.22 μm) using a 25 mm outer diameter glass filter frit and a vacuum filter holder. An unoxidized PDMS carrier substrate was then brought into contact with the filter paper with slight pressure. Peeling off the filter paper transferred the AgNW film to the PDMS carrier surface. AgNW films on PDMS carriers were annealed at 200 °C for 20 min on a hot plate, cooled to room temperature, and then cut to the desired size/geometry (1 cm × 1 cm square for transmittance and sheet resistance, 1.5 cm × 0.2 cm strips for bending experiments, and 1.5 cm diameter circles for durability testing and LEEC fabrication) using a scalpel. A drop (5 μL/cm^2 of AgNW film) of optical adhesive (NOA 83H, Norland Optical) was then placed

onto the surface of the AgNW film, and the target substrate (glass, PET, or oxidized PDMS) was placed on top. The adhesive was allowed to spread for 1 min and then was cured under a 100 W mercury lamp for 15 min. The PDMS carrier was then removed, leaving the AgNW-OA coating on the target substrate.

Fabrication of LEECs. AgNW-OA anodes were oxidized in an oxygen plasma for 45 s, and a PEDOT:PSS (Heraeus Clevios P) layer was spin-coated at 1000 rpm for 1 min on the surface by sonicating aqueous PEDOT:PSS dispersion for 15 min, heating the dispersion to 90 °C for 15 min, and diluting with 30% isopropanol. The PEDOT:PSS film was annealed on a hot plate at 100 °C for 20 min. After cooling to room temperature, a $Ru(dtb\text{-}bpy)_3(PF_6)_2$/PMMA emissive layer was deposited by spin-coating a 3:1 v/v mixture of a 40 mg/mL solution of $Ru(dtb\text{-}bpy)_3(PF_6)_2$ in acetonitrile and a 25 mg/mL solution of PMMA (Avg M_W = 120 000) at 1500 rpm for 30 s. The film was annealed in a vacuum oven at 120 °C overnight. A eutectic gallium indium (EGaIn) cathode was deposited onto the surface of the Ru/PMMA film using a syringe and then sealed in epoxy resin.

Characterization. Optical inspection was performed using an Olympus BX51 microscope equipped with an Olympus Q-Color3 camera. SEM images were collected with a Hitachi S-4500 field emission SEM (Surface Science Western, London, ON, Canada). AFM images (40 μm × 40 μm) were collected using the dynamic force mode of a Park Systems XE-100 AFM (Surface Science Western). AFM images (10 μm × 10 μm) were collected using the tapping mode of a Digital Instruments Multimode AFM. Transmittance spectra were recorded using a Varian Cary 50 UV-Visible spectrophotometer. Sheet resistance values were measured using the four-point probe technique with a Keithley 2601 source meter and EGaIn contacts, with a minimum of three measurements for each sample. Bending experiments were performed by wrapping AgNW-OA films on PET or oxidized PDMS around cylindrical objects with radii varying from 13.5 to 0.65 mm and measuring the resistance of the film at each bending radius. A minimum of three measurements were averaged for each radius. AgNW-OA films on PET were subjected to high tensile strain by manually creasing the PET sheet to a radius of ~0.1 mm as measured by optical microscopy. The adhesive tape test was performed by measuring the resistance of the AgNW-OA film on PDMS before and after adhering and peeling off a 1 cm × 2 cm piece of tape (Permacel). The finger friction test was performed by measuring the resistance of a AgNW-OA film on PDMS before and after continuous rubbing with a gloved finger for 30 s. The solvent durability test was performed by measuring the resistance of the AgNW-OA film on PDMS before and after immersion into H_2O and EtOH for 6 h. EGaIn contacts were removed using a scalpel prior to solvent immersion. After immersion, new EGaIn contacts were placed onto the film, and the resistance was normalized to the new length. The repetitive clamping test was performed by measuring the resistance of the AgNW-OA and ITO films on glass after a number of clamping and unclamping cycles of the same area of the film with alligator clips. LEEC devices were characterized using a Keithley 2601 source-measure unit to apply a DC bias voltage and measure the current. Radiance was measured with a calibrated UDT S470 optometer attached to an integrating sphere.

AUTHOR INFORMATION

Corresponding Author

*E-mail: tbcarmic@uwindsor.ca.

Notes

The authors declare no competing financial interest.

ACKNOWLEDGMENTS

This research was supported by the National Sciences and Engineering Research Council of Canada (NSERC). M.S.M. is grateful for the award of an NSERC post-graduate doctoral scholarship (CGSD).

REFERENCES

(1) Mone, G. *Commun. ACM* **2013**, *56*, 16−17.
(2) Cairns, D. R.; Crawford, G. P. *Proc. IEEE* **2005**, *93*, 1451−1458.
(3) Lewis, B. G.; Paine, D. C. *MRS Bull.* **2000**, *25*, 22−27.
(4) Cao, Q.; Rogers, J. A. *Adv. Mater.* **2009**, *21*, 29−53.
(5) Becerril, H. A.; Mao, J.; Liu, Z.; Stoltenberg, R. M.; Bao, Z.; Chen, Y. *ACS Nano* **2008**, *2*, 463−470.
(6) Eda, G.; Fanchini, G.; Chhowalla, M. *Nat. Nanotechnol.* **2008**, *3*, 270−274.
(7) Chang, Y.-M.; Wang, L.; Su, W.-F. *Org. Electron.* **2008**, *9*, 968−973.
(8) Colsmann, A.; Stenzel, F.; Balthasar, G.; Do, H.; Lemmer, U. *Thin Solid Films* **2009**, *517*, 1750−1752.
(9) Do, H.; Reinhard, M.; Vogeler, H.; Puetz, A.; Klein, M. F. G.; Schabel, W.; Colsmann, A.; Lemmer, U. *Thin Solid Films* **2009**, *517*, 5900−5902.
(10) Krebs, F. C. *Org. Electron.* **2009**, *10*, 761−768.
(11) Krebs, F. C. *Sol. Energy Mater. Sol. Cells* **2009**, *93*, 1636−1641.
(12) Galagan, Y.; Rubingh, J.-E. J. M.; Andriessen, R.; Fan, C.-C.; Blom, P. W. M.; Veenstra, S. C.; Kroon, J. M. *Sol. Energy Mater. Sol. Cells* **2011**, *95*, 1339−1343.
(13) Kang, M.-G.; Kim, M.-S.; Kim, J.; Guo, L. J. *Adv. Mater.* **2008**, *20*, 4408−4413.
(14) Gaynor, W.; Burkhard, G. F.; McGehee, M. D.; Peumans, P. *Adv. Mater.* **2011**, *23*, 2905−2910.
(15) Lee, J. Y.; Connor, S. T.; Cui, Y.; Peumans, P. *Nano Lett.* **2008**, *8*, 689−692.
(16) Madaria, A. R.; Kumar, A.; Ishikawa, F. N.; Zhou, C. W. *Nano Res.* **2010**, *3*, 564−573.
(17) Liu, C. H.; Yu, X. *Nanoscale Res. Lett.* **2011**, *6*, 75.
(18) Hu, L. B.; Kim, H. S.; Lee, J. Y.; Peumans, P.; Cui, Y. *ACS Nano* **2010**, *4*, 2955−2963.
(19) Scardaci, V.; Coull, R.; Lyons, P. E.; Rickard, D.; Coleman, J. N. *Small* **2011**, *7*, 2621−2628.
(20) Akter, T.; Kim, W. S. *ACS Appl. Mater. Interfaces* **2012**, *4*, 1855−1859.
(21) De, S.; Higgins, T. M.; Lyons, P. E.; Doherty, E. M.; Nirmalraj, P. N.; Blau, W. J.; Boland, J. J.; Coleman, J. N. *ACS Nano* **2009**, *3*, 1767−1774.
(22) Lee, P.; Lee, J.; Lee, H.; Yeo, J.; Hong, S.; Nam, K. H.; Lee, D.; Lee, S. S.; Ko, S. H. *Adv. Mater.* **2012**, *24*, 3326−3332.
(23) Azulai, D.; Belenkova, T.; Gilon, H.; Barkay, Z.; Markovich, G. *Nano Lett.* **2009**, *9*, 4246−4249.
(24) Yang, L. Q.; Zhang, T.; Zhou, H. X.; Price, S. C.; Wiley, B. J.; You, W. *ACS Appl. Mater. Interfaces* **2011**, *3*, 4075−4084.
(25) Zeng, X. Y.; Zhang, Q. K.; Yu, R. M.; Lu, C. Z. *Adv. Mater.* **2010**, *22*, 4484−4488.
(26) Hu, W.; Niu, X.; Li, L.; Yun, S.; Yu, Z.; Pei, Q. *Nanotechnology* **2012**, *23*, 344002.
(27) Yu, Z. B.; Zhang, Q. W.; Li, L.; Chen, Q.; Niu, X. F.; Liu, J.; Pei, Q. B. *Adv. Mater.* **2011**, *23*, 664−668.
(28) Xu, F.; Zhu, Y. *Adv. Mater.* **2012**, *24*, 5117−5122.
(29) Leem, D. S.; Edwards, A.; Faist, M.; Nelson, J.; Bradley, D. D.; de Mello, J. C. *Adv. Mater.* **2011**, *23*, 4371−4375.
(30) Li, L.; Yu, Z.; Hu, W.; Chang, C. H.; Chen, Q.; Pei, Q. *Adv. Mater.* **2011**, *23*, 5563−5567.
(31) Rathmell, A. R.; Wiley, B. J. *Adv. Mater.* **2011**, *23*, 4798−4803.
(32) Burrows, P. E.; Graff, G. L.; Gross, M. E.; Martin, P. M.; Shi, M. K.; Hall, M.; Mast, E.; Bonham, C.; Bennett, W.; Sullivan, M. B. *Displays* **2001**, *22*, 65−69.
(33) The static water contact angle of native PDMS was measured to be 114°. The static water contact angle of glass, PET, and oxidized PDMS were measured to be <10°, 77°, and <10°, respectively.
(34) AgNW films made by drop-casting an identical AgNW volume and concentration on glass had a $\%T_{550nm}$ = 89.6.
(35) Lewis, J. *Mater. Today* **2006**, *9*, 38−45.
(36) Xu, F.; Durham, J. W.; Wiley, B. J.; Zhu, Y. *ACS Nano* **2011**, *5*, 1556−1563.

(37) Jin, L.; Bower, C.; Zhou, O. *Appl. Phys. Lett.* **1998**, *73*, 1197−1199.
(38) Iakoubovskii, K. *Cent. Eur. J. Phys.* **2009**, *7*, 645−653.
(39) Slinker, J. D.; Rivnay, J.; Moskowitz, J. S.; Parker, J. B.; Bernhard, S.; Abruna, H. D.; Malliaras, G. G. *J. Mater. Chem.* **2007**, *17*, 2976−2988.
(40) Pei, Q. B.; Yu, G.; Zhang, C.; Yang, Y.; Heeger, A. J. *Science* **1995**, *269*, 1086−1088.
(41) Lenes, M.; Garcia-Belmonte, G.; Tordera, D.; Pertegas, A.; Bisquert, J.; Bolink, H. J. *Adv. Funct. Mater.* **2011**, *21*, 1581−1586.
(42) Slinker, J. D.; DeFranco, J. A.; Jaquith, M. J.; Silveira, W. R.; Zhong, Y. W.; Moran-Mirabal, J. M.; Craighead, H. G.; Abruna, H. D.; Marohn, J. A.; Malliaras, G. G. *Nat. Mater.* **2007**, *6*, 894−899.
(43) deMello, J. C. *Phys. Rev. B* **2002**, *66*, 235210.
(44) Rodovsky, D. B.; Reid, O. G.; Pingree, L. S. C.; Ginger, D. S. *ACS Nano* **2010**, *4*, 2673−2680.
(45) Filiatrault, H. L.; Porteous, G. C.; Carmichael, R. S.; Davidson, G. J. E.; Carmichael, T. B. *Adv. Mater.* **2012**, *24*, 2673−2678.
(46) Yu, Z. B.; Niu, X. F.; Liu, Z. T.; Pei, Q. B. *Adv. Mater.* **2011**, *23*, 3989−3994.
(47) Yu, Z. B.; Hu, L. B.; Liu, Z. T.; Sun, M. L.; Wang, M. L.; Gruner, G.; Pei, Q. B. *Appl. Phys. Lett.* **2009**, *95*, 203304.
(48) Slinker, J. D.; Kim, J. S.; Flores-Torres, S.; Delcamp, J. H.; Abruna, H. D.; Friend, R. H.; Malliaras, G. G. *J. Mater. Chem.* **2007**, *17*, 76−81.
(49) Bernards, D. A.; Biegala, T.; Samuels, Z. A.; Slinker, J. D.; Malliaras, G. G.; Flores-Torres, S.; Abruna, H. D.; Rogers, J. A. *Appl. Phys. Lett.* **2004**, *84*, 3675−3677.